Supporting Information for "Bayesian updating on time intervals at different magnitude thresholds in a marked point process and its application to synthetic seismic activity"

Hiroki Tanaka [1]and Ken Umeno [1]

[1]Kyoto University, Yoshida-honmachi, Sakyo-ku, Kyoto-shi, JAPAN

Contents of this file

1. Figures S1 to S17

Introduction The following figures are provided in this supporting information. Figure S1–S7 present information regarding the numerically generated uncorrelated time series. Figure S1 shows the probability density functions of the length of the inter-event times ($p_m(\tau_m)$ and $p_M(\tau_M)$) and their interpolation and extrapolation functions. Figure S2 shows the conditional probability density function of the length of the lower intervals included in the upper interval of length τ_M ($p_{mM}(\tau_m|\tau_M)$) and its interpolation and extrapolation functions. Figure S3 shows the conditional probability density function of the length of the left-most lower interval included in the upper interval of length τ_M ($P_1(\tau_m|\tau_M)$) and its interpolation and extrapolation functions. Figure S4 shows the average number of lower intervals included in the upper interval of length τ_M ($\tau_M/\langle\langle\tau_m\rangle\rangle_{\tau_M}$) and its interpolation and extrapolation functions. Figure S5 shows an example of Bayesian

updating. Figure S6 shows the average distances between the distribution functions and the (part of) approximation functions including the results of numerical Bayesian updating using statistical amounts calculated using the $\mathcal{N} = 10^5$ time series. Figure S7 shows the joint probability mass function of the logarithm of the positions of the maximum peak of the inverse probability density function and its approximation function calculated by numerical Bayesian updating with $\mathcal{N} = 10^5$. Figures S8–S17 are about the numerically generated time series of the ETAS model. Figure S8 shows $p_m(\tau_m)$ and $p_M(\tau_M)$, and their interpolation and extrapolation functions. Figure S9 shows $p_{mM}(\tau_m|\tau_M)$ and its interpolation and extrapolation functions. Figure S10 and S11 show the conditional probability density functions of the left-most and right-most lower intervals included in the upper interval of length τ_M ($p^{\mathrm{L}}(\tau_m|\tau_M)$ and $p^{\mathrm{R}}(\tau_m|\tau_M)$, respectively) and their interpolation and extrapolation functions. Figure S12 shows $\tau_M/\langle\langle\tau_m\rangle\rangle_{\tau_M}$ and its interpolation and extrapolation functions. Figure S13–S15 show examples of Bayesian updating for $\delta_{\mathrm{th}} = 0.5$. Figure S16 shows the probability density functions of $n_{\leq\mathrm{th}}$ and $\tau_{\leq\mathrm{th}}$ for $\delta_{\mathrm{th}} = 0.5$. Figure S17 shows the statistical results of the effectiveness of forecasting for $\delta_{\mathrm{th}} = 0.25$.

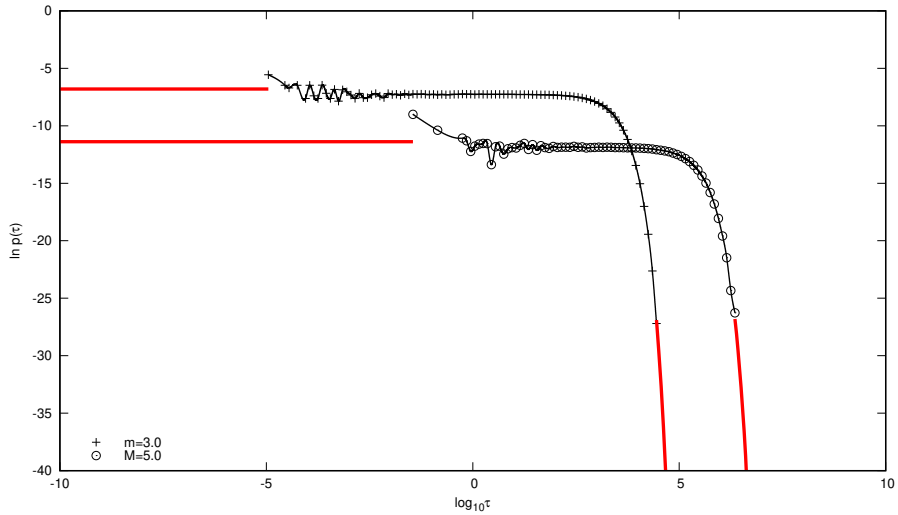

Figure S1. Probability density functions of the length of inter-event times at magnitude thresholds $m = 3.0$ and $M = 5.0$ calculated for the numerically generated uncorrelated time series, and their interpolation and extrapolation functions. Symbols ($+$ and $\odot$) show the probability density functions obtained numerically. The intervals between the symbols are interpolated by cubic spline functions represented by the black curves. Further, outside of the range covered by the symbols are extrapolated by the fitting functions at the edge represented by the red lines; constant function ($\ln p(\tau) \equiv C$) on the small side and the exponential function ($\ln p(\tau) = A\tau + B$) on the large side. The parameter values (A, B, C) are determined by the least squares method using 10 points at each end.

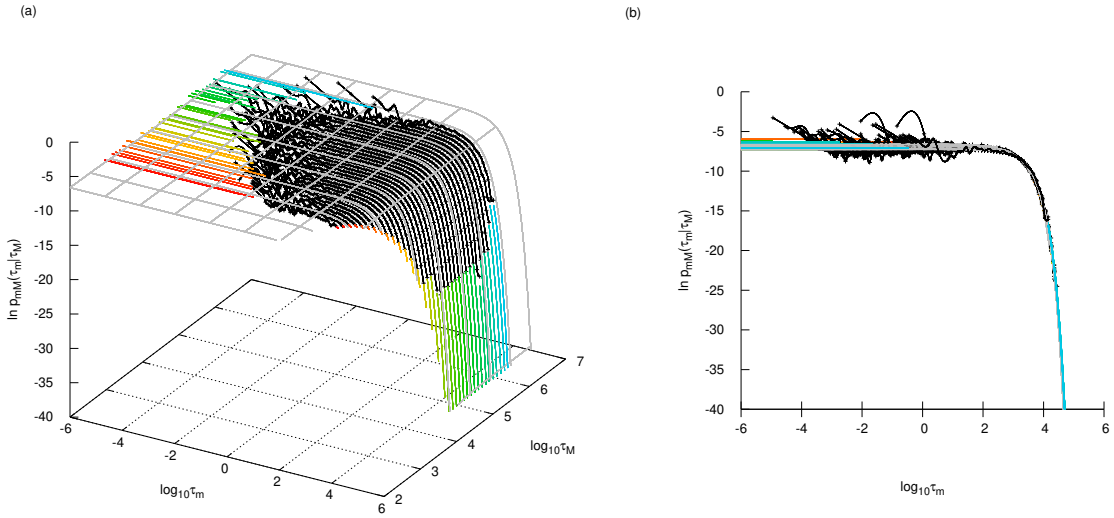

Figure S2. Conditional probability density function of the length of the lower interval (τ_m) included in the upper interval of length τ_M for the uncorrelated time series, and its interpolation and extrapolation functions in (a) an oblique view and (b) a horizontal view parallel to the $\log_{10}\tau_M$-axis. Gray curved surface is the part of the step function of Equation (15). Symbols (+) represent the probability density function obtained numerically. For each τ_M, only data points with 30 or more points in the range of $\tau_M > \tau_m$ are displayed. The intervals between the symbols in the $\log_{10}\tau_m$-axis direction are interpolated by cubic spline functions represented by the black curves. Outsides of the range covered by the symbols in the $\log_{10}\tau_m$-axis direction are extrapolated by the fitting functions at the edge represented by the colored lines (the color varies with $\log_{10}\tau_M$); constant function ($\ln p(\tau) \equiv C$) on the small τ_m side and the exponential function ($\ln p(\tau) = A\tau + B$) on the large τ_m side for each τ_M. The parameter values (A, B, C) are determined by the least squares method using 10 points at each end for each τ_M.

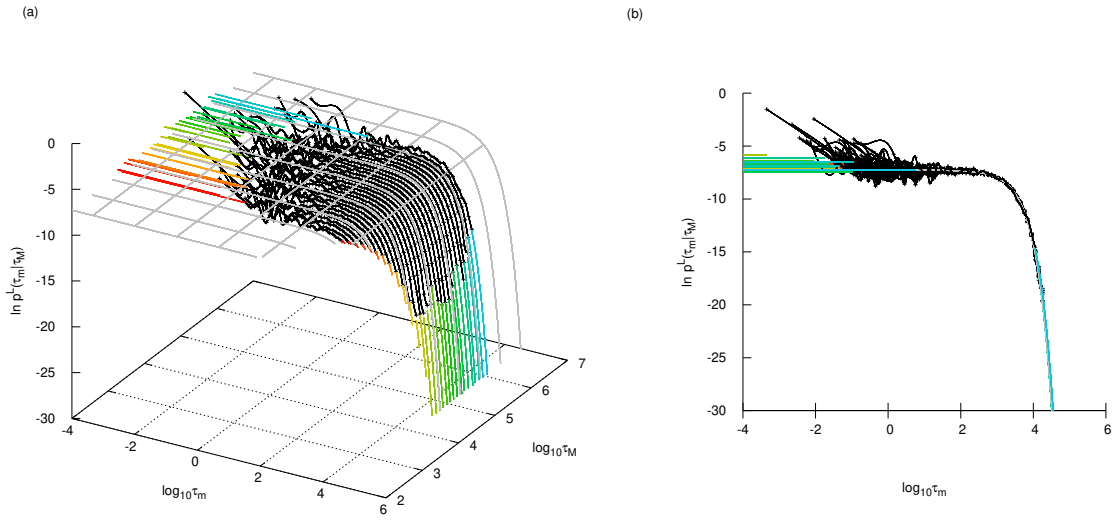

Figure S3. Conditional probability density function of the length of the left-most lower interval included in the upper interval of length τ_M for the uncorrelated time series, and its interpolation and extrapolation functions in (a) an oblique view and (b) a horizontal view parallel to the $\log_{10}\tau_M$-axis. Gray curved surface shows the part of the step function of Equation (29). The description of the figure is the same as in Figure S2.

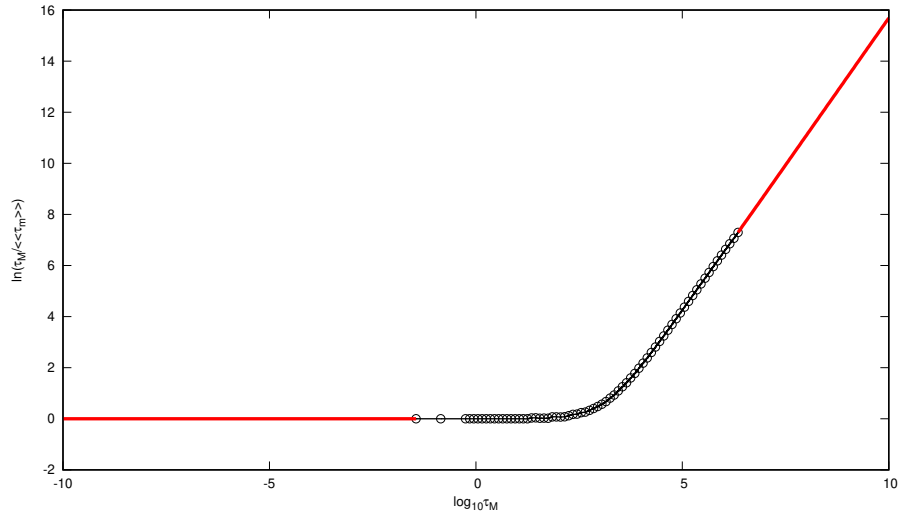

Figure S4. Average number of lower intervals included in the upper interval of length τ_M ($\tau_M/\langle\langle\tau_M\rangle\rangle_{\tau_M}$) for the uncorrelated time series, and its interpolation and extrapolation functions. Symbols ($\odot$) indicate the results obtained numerically. The intervals between the symbols are interpolated by cubic spline functions represented by the black curves. Outsides of the range covered by the symbols are replaced or extrapolated by following functions represented by red lines; $\ln \tau_M/\langle\langle\tau_M\rangle\rangle_{\tau_M} \equiv 0$ on the small side, whereas the fitting function $\tau_M/\langle\langle\tau_M\rangle\rangle_{\tau_M} = A\tau_M + B$ on the large side with the parameter values determined by the least squares method using 10 points at the end.

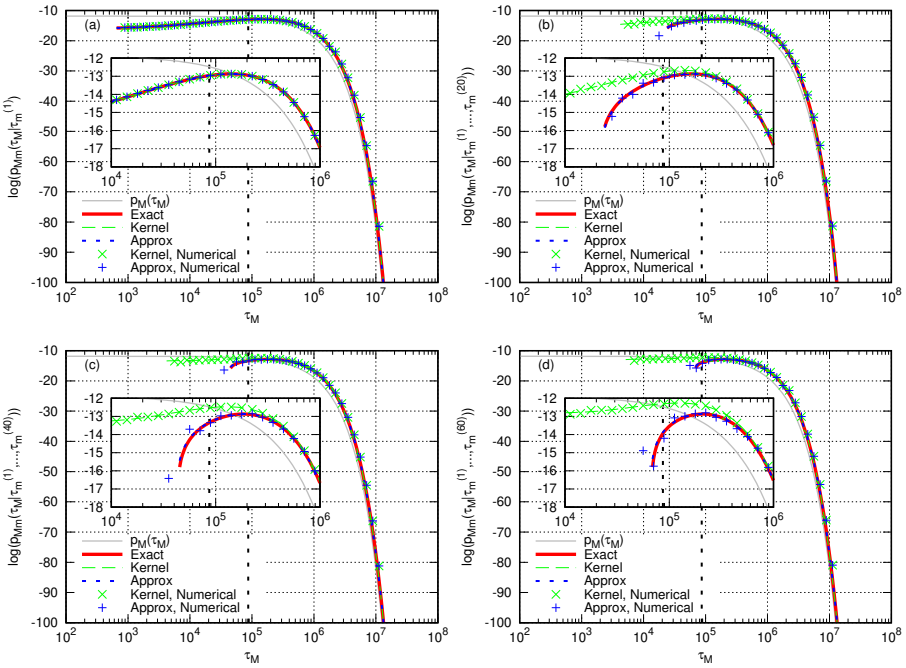

Figure S5. Examples of the Bayesian updating on a numerically generated uncorrelated time series. In this example, the total number of updates between the events with a magnitude above M is 73. The horizontal axis represents the elapsed time from the previous event with a magnitude above M, and the vertical axis is the logarithmic scale of the inverse probability density function and its approximation function for n = (a) 1, (b) 20, (c) 40, and (d) 60, respectively. Gray curve is $p_M(\tau_M)$ and black vertical dotted line indicates the actual elapsed time of the next large event with a magnitude above M. At each update, (Exact) the inverse probability density function (Equation (24)), (Approx) the approximation function (Equation (39)), and (Kernel) its kernel part (Equation (40)) are shown. Further, the results with the numerical updating method (Equations (43) and (44)) are shown for the approximation function and its kernel part; (Kernel, Numerical) represents the result of Equation (43), and (Approx, Numerical) is for Equations (43) and (44).

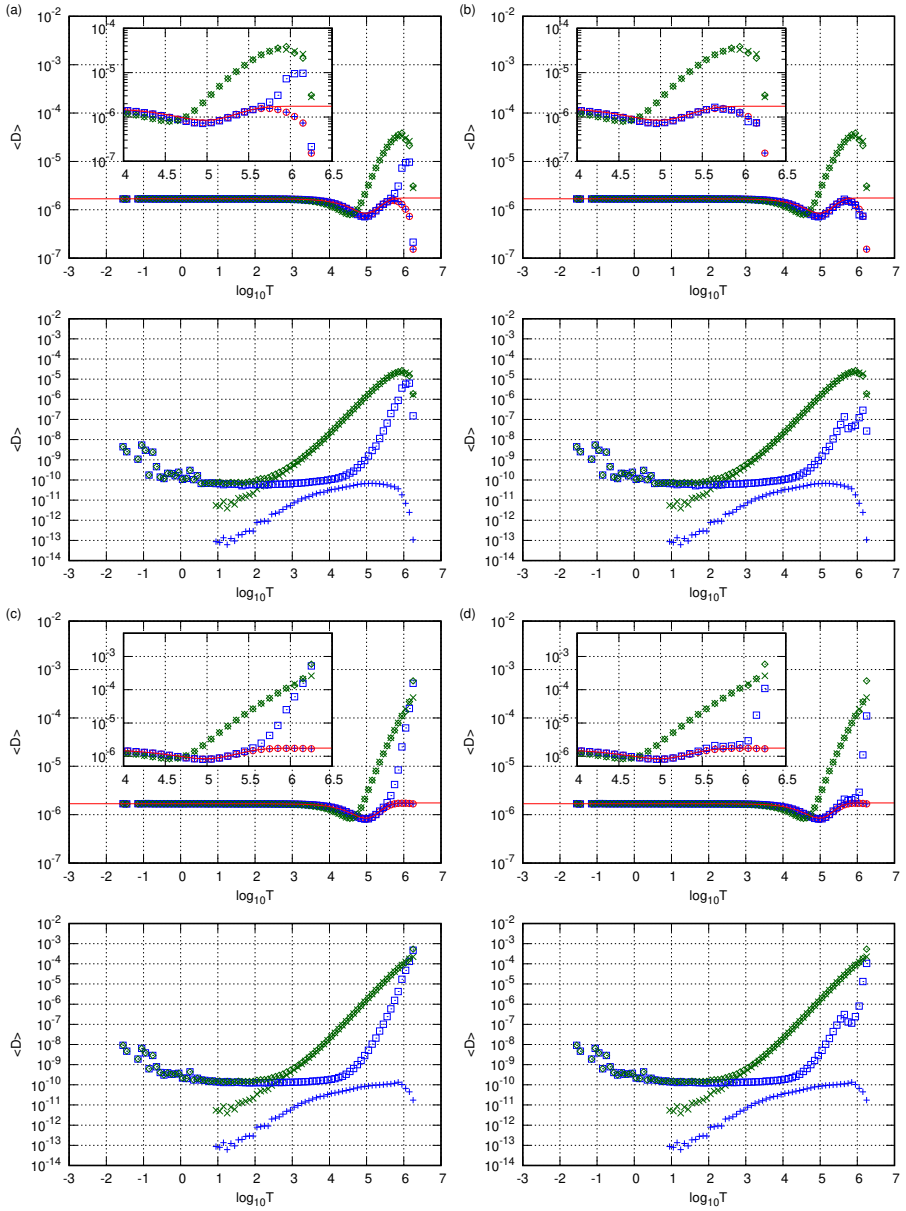

Figure S6. Average distances for elapsed time T from the last event greater than M. Each symbol represents the same distance as in Figure 7. The results of the numerical updating of $\langle D'' \rangle$ are calculated using statistical amounts in Equation (42) taken from the $\mathcal{N} = 10^5$ time series with (a) $\Delta\tau_M = 0.1$ and $l_c = 0$, (b) $\Delta\tau_M = 0.1$ and $l_c = 5$, (c) $\Delta\tau_M = 0.025$ and $l_c = 0$, and (d) $\Delta\tau_M = 0.025$ and $l_c = 20$.

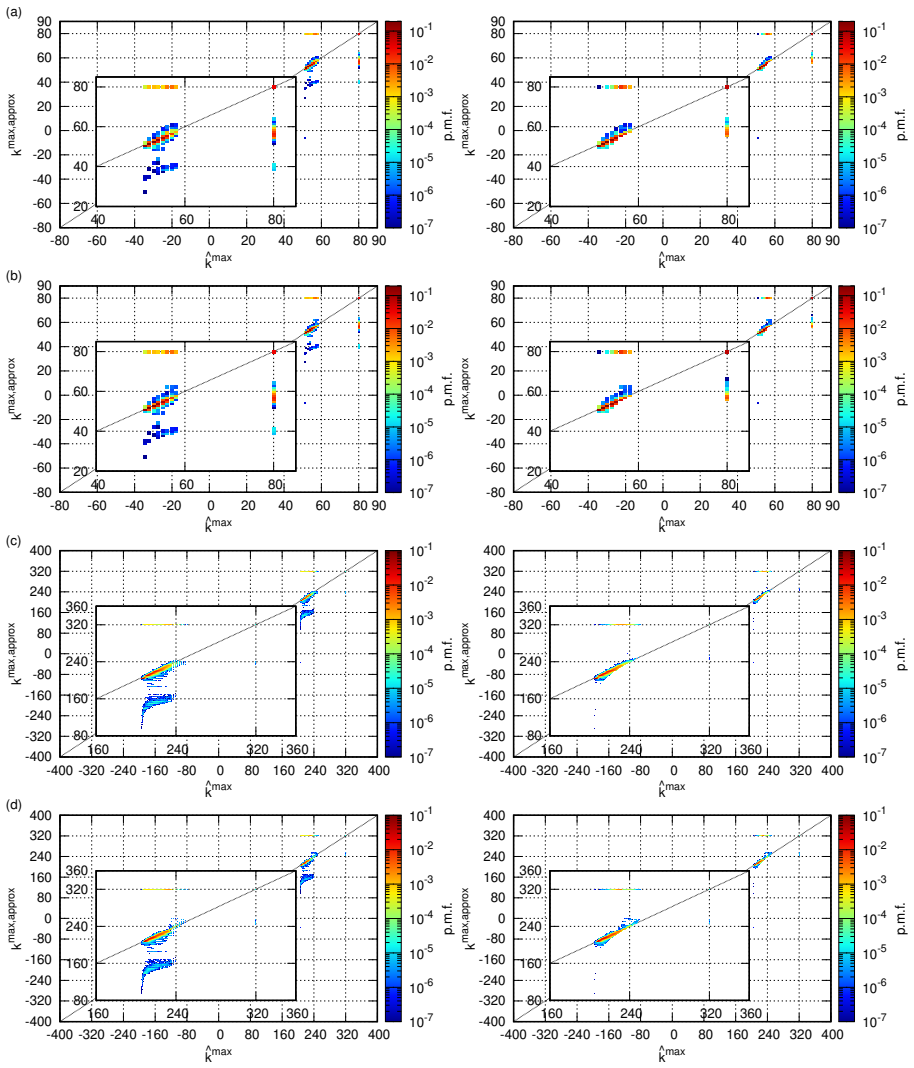

Figure S7. Joint probability mass function of $(\hat{k}^{\max}, k^{\max,\text{approx}})$. $k^{\max,\text{approx}}$ is obtained using the numerical updating method with statistical amounts in Equation (42) taken from the $\mathcal{N} = 10^5$ time series with (a) $\Delta\tau_M = 0.1$ and $l_c = 0$, (b) $\Delta\tau_M = 0.1$ and $l_c = 5$, (c) $\Delta\tau_M = 0.025$ and $l_c = 0$, and (d) $\Delta\tau_M = 0.025$ and $l_c = 20$. For (a) and (b), the horizontal lines at $k^{\max,\text{approx}} = 80$ and the vertical line at $\hat{k}^{\max} = 80$ correspond to cases when no peak is detected by the peak search. Further, for (c) and (d), the lines at $k^{\max,\text{approx}} = 320$ and at $\hat{k}^{\max} = 320$ correspond to the no peak cases. The left panels are results when the peak search is conducted in the range of $\tau_M > \max\{\tau_m^{(1)}, \cdots, \tau_m^{(n)}\}$ and the right panels in the range of $\tau_M > T$.

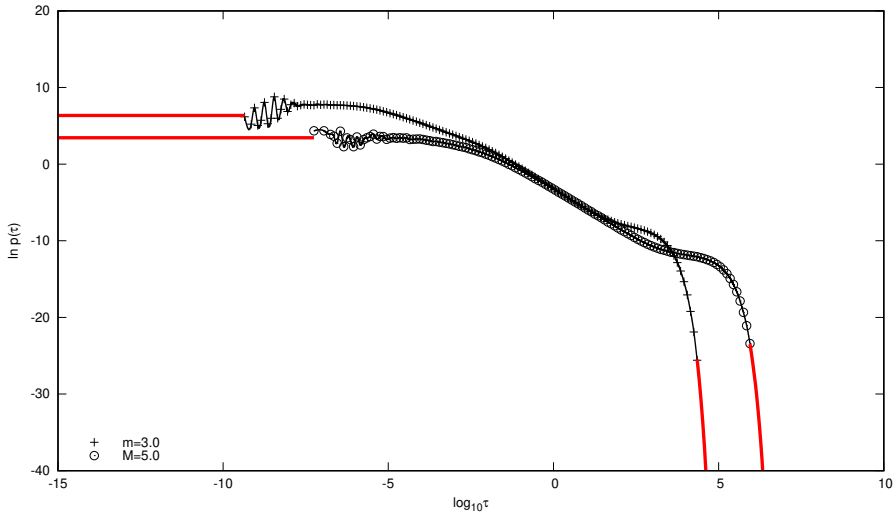

Figure S8. Probability density functions of the length of inter-event times at magnitude thresholds $m = 3.0$ and $M = 5.0$ calculated for the numerically generated time series of the ETAS model, and their interpolation and extrapolation functions. The description of the figure is the same as in Figure S1.

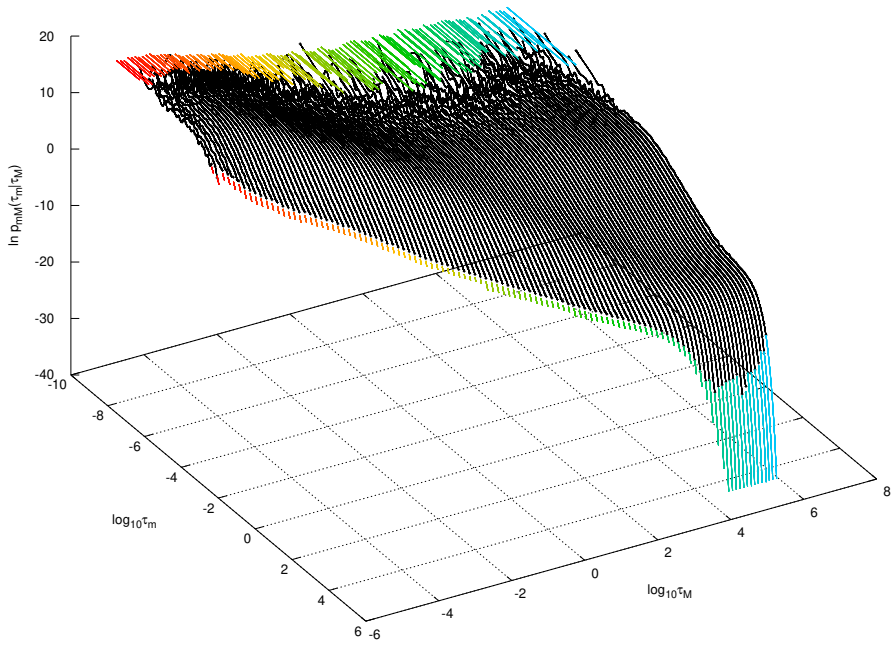

Figure S9. Conditional probability density function of the length of the lower interval (τ_m) included in the upper interval of length τ_M for the numerically generated time series of the ETAS model, and its interpolation and extrapolation functions. The description of the figure is the same as in Figure S2.

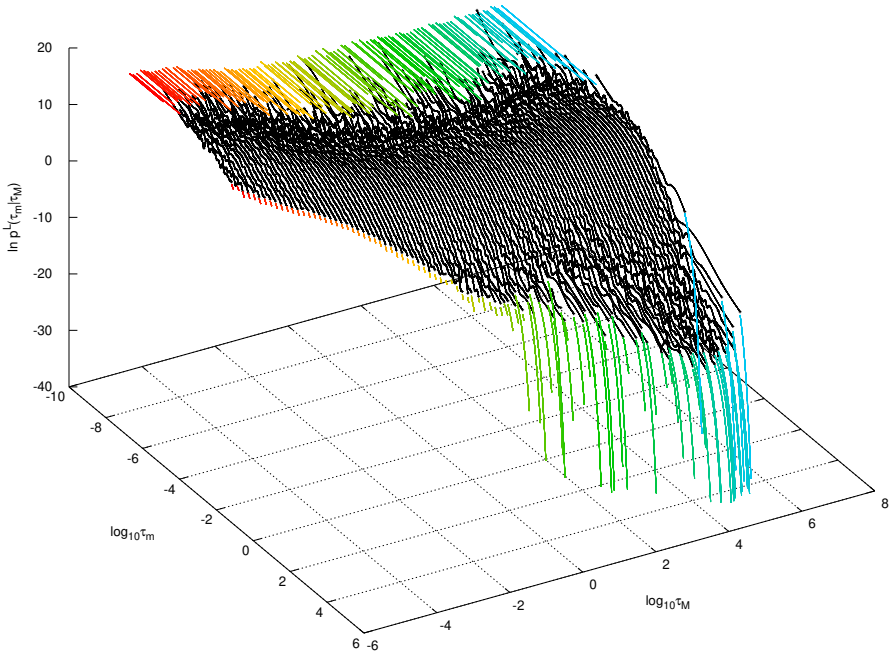

Figure S10. Conditional probability density function of the length of the left-most lower interval included in the upper interval of length τ_M for the numerically generated time series of the ETAS model, and its interpolation and extrapolation functions. The description of the figure is the same as in Figure S3.

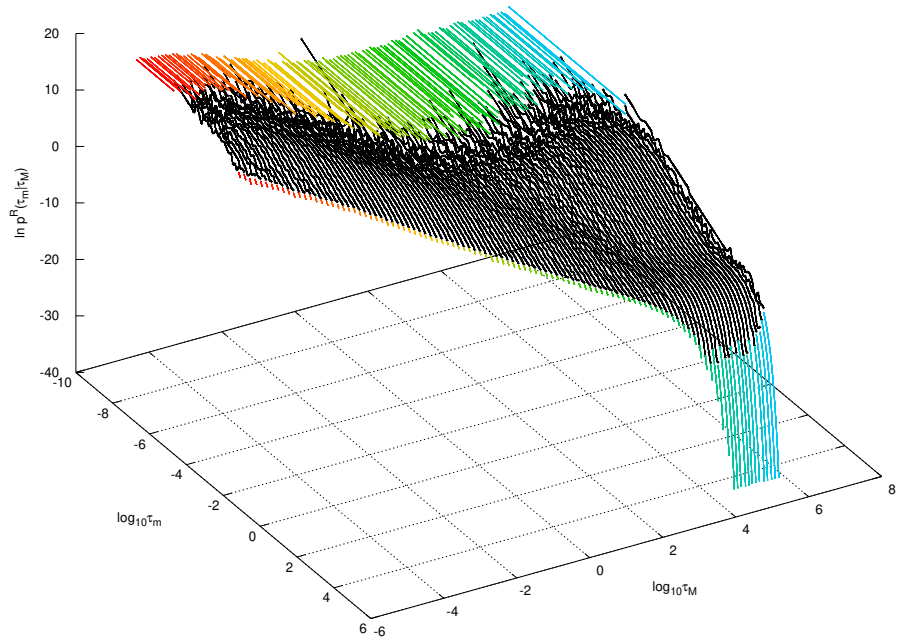

Figure S11. Conditional probability density function of the length of the right-most lower interval included in the upper interval of length τ_M for the numerically generated time series of the ETAS model, and its interpolation and extrapolation functions. The description of the figure is the same as in Figure S3.

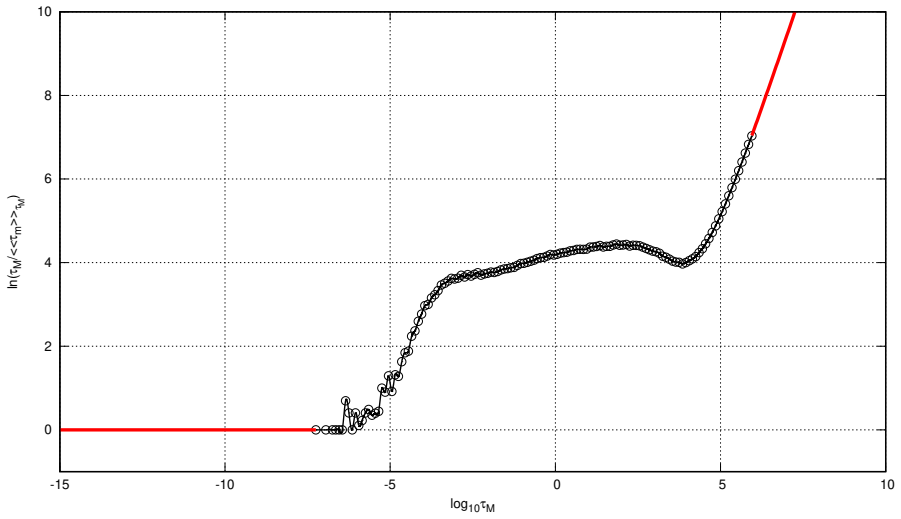

Figure S12. Average number of lower intervals included in the upper interval of length τ_M ($\tau_M/\langle\langle\tau_M\rangle\rangle_{\tau_M}$) for the numerically generated time series of the ETAS model. The description of the figure is the same as in Figure S4.

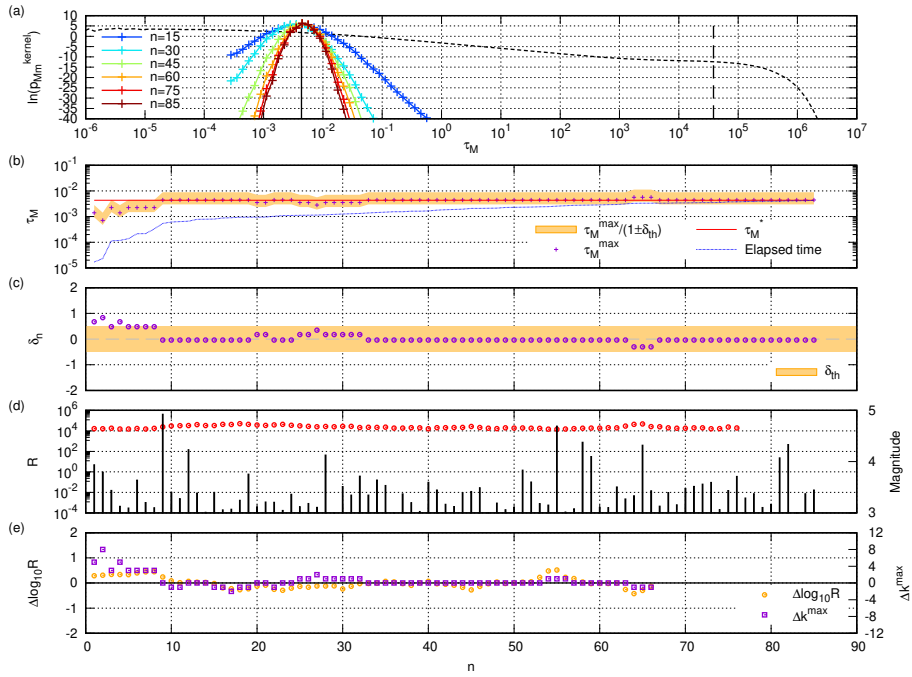

Figure S13. First example of Bayesian updating. This is the case where τ_M^* is in regime (I). (a) Around the peak of the kernel part for each update. The dotted curve indicates $p_M(\tau_M)$. (b) Evolutions of the estimate ($\tau_M^{\max,\mathrm{n}}$) and the tolerance of error $\left[\frac{\tau_M^{\max,\mathrm{n}}}{1+\delta_{\mathrm{th}}}, \frac{\tau_M^{\max,\mathrm{n}}}{1-\delta_{\mathrm{th}}}\right]$ in Equation (50) with $\delta_{\mathrm{th}} = 0.5$. The elapsed time from the last large event is indicated by the dotted line. (c) Evolution of the relative error (δ_n). The orange band indicates the tolerance range $\pm\delta_{\mathrm{th}}$. (d) Evolution of the occurrence rate (R_n defined by Equation (51)). The magnitude of the event at each update is indicated by black bars. (e) Evolutions of the variation of the log-occurrence rate ($\Delta \log_{10} R_n$ defined by Equation (52)) and the variation of the log-estimate ($\Delta k_n^{\max}$ defined by Equation (53)). In this example, the occurrence rate is high, and it stays almost constant as shown in (d). The kernel part has a peak as shown in (a). Its maximum peak time ($\tau_M^{\max,\mathrm{n}}$) continues to be nearly constant around τ_M^* from well before the large event as shown in (b); this is confirmed in (c), which indicates that $|\delta_n| \leq \delta_{\mathrm{th}}$ is satisfied consecutively for $n \in (n_{\mathrm{fin}} - n_{\leq \mathrm{th}}, n_{\mathrm{fin}}]$ with a long $n_{\leq \mathrm{th}}$, and in (e), that shows that $\Delta k_n^{\max}$ fluctuate around 0. Then, in this example, τ_M^* is judged to be effectively forecasted for the setting of $\delta_{\mathrm{th}} = 0.5$.

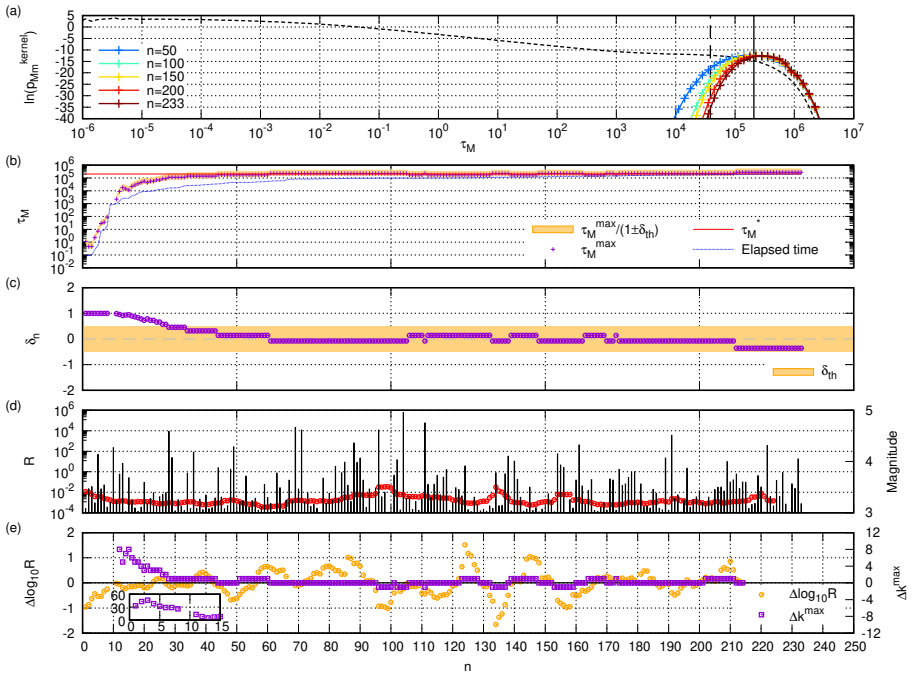

Figure S14. Second example of Bayesian updating. This is the case that τ_M^* is in regime (Ⅲ). In some cases, the kernel part does not have the maximum peak, and the estimate is not determined, which causes some jumps in the time series. The inset in (e) shows $\Delta k_n^{\max}$ for small number of updates, indicating a rapid variation of $k^{\max,\mathrm{n}}$ at small n. Other descriptions of the figure is the same as in Figure S13. In this example, the occurrence rate is low and keeps almost constant around $\lambda_0 = 0.0007$, as shown in (d). (b) and (c) show that the maximum peak time of the kernel part ($\tau_M^{\max,\mathrm{n}}$) transitions to around τ_M^*, and it consecutively satisfies $|\delta_n| \leq \delta_{\mathrm{th}} = 0.5$ from long to immediately before the next large event. Further, this is also confirmed by $\Delta k_n^{\max} \approx 0$ in (e). Therefore, in this example, the forecasting is judged to be conducted effectively.

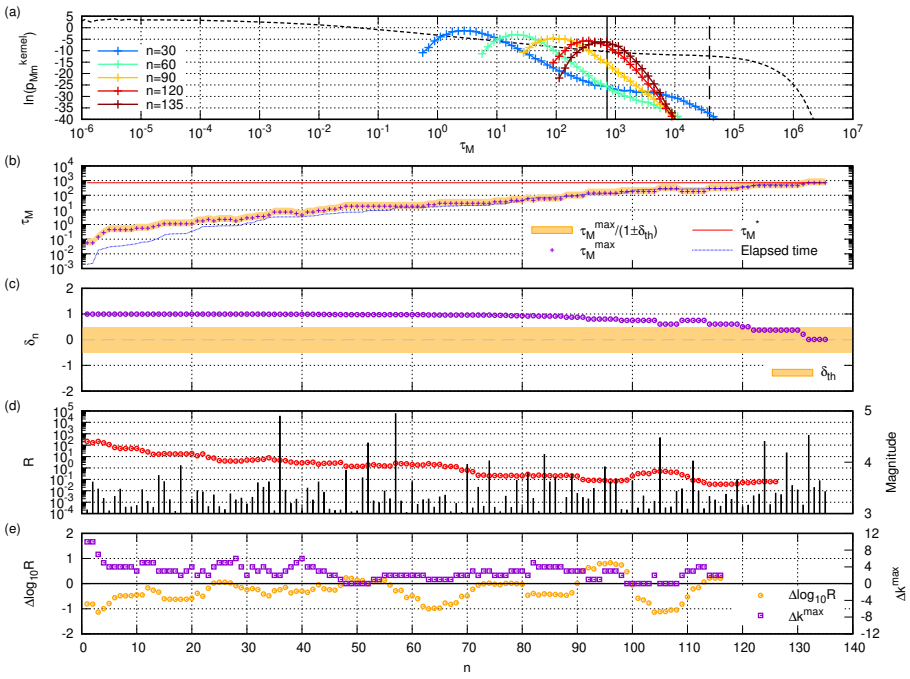

Figure S15. Third example of Bayesian updating. This is the case that τ_M^* is in regime (II). The descriptions of the figure are the same as in Figure S13. In this example, unlike in Figures S13 and S14, the time series is dominated by the non-stationary activity as shown in (d) and (e). Although $|\delta_n| \leq \delta_{\rm th} = 0.5$ is satisfied only immediately before the large shock, $\tau_M^{\rm max,n}$ continues shifting and $|\delta_n| \leq \delta_{\rm th}$ does not hold as shown in (b), (c), and (e). Therefore, the forecasting is not effective in this case.

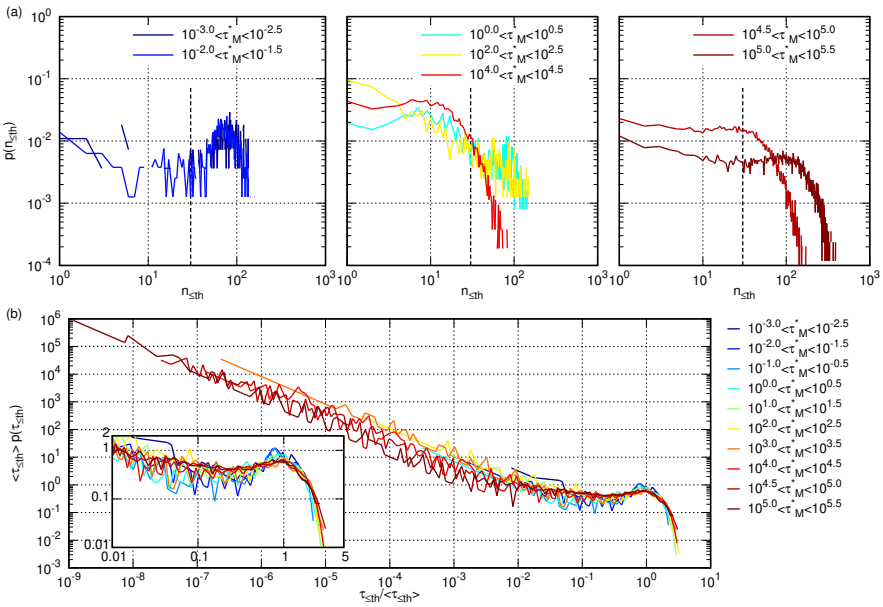

Figure S16. (a) Probability distributions ($p(n_{\leq \mathrm{th}})$) of the number of consecutive updates ($n_{\leq \mathrm{th}}$) with $|\delta_n| \leq \delta_{\mathrm{th}} = 0.5$ for each τ_M^*. Only the cases with $n_{\leq \mathrm{th}} > 0$ are included in the population. The vertical dotted line indicates $n_{\leq \mathrm{th}} = 30$. (b) Probability density function ($p(\tau_{\leq \mathrm{th}})$) of the duration time ($\tau_{\leq \mathrm{th}}$) during n_{th}-updates with $\delta_{\mathrm{th}} = 0.5$ for each τ_M^*. The distributions rescaled by the averages ($\langle \tau_{\leq \mathrm{th}} \rangle := \int_0^\infty \tau_{\leq \mathrm{th}} p(\tau_{\leq \mathrm{th}}) d\tau_{\leq \mathrm{th}}$) are shown.

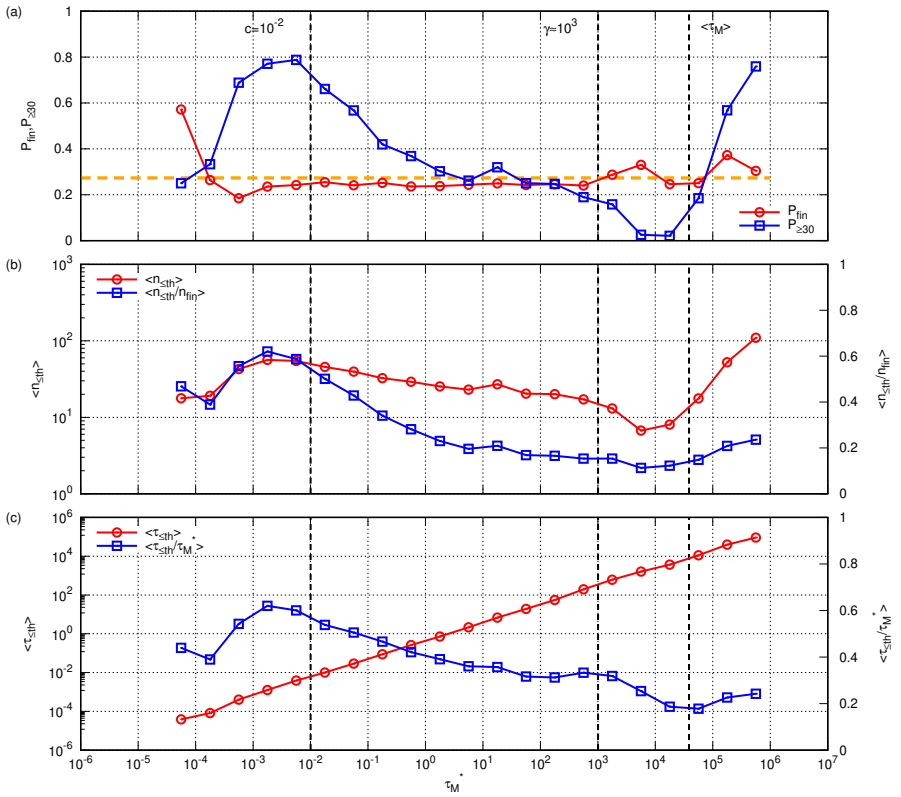

Figure S17. Statistical results for each τ_M^* with $\delta_{\rm th} = 0.25$. (a) $P_{\rm fin}$, $P_{\geq 30}$, and the average of $P_{\rm fin}(\approx 0.27)$ for the overall τ_M^*; (b) $\langle n_{\leq {\rm th}} \rangle$ and $\langle n_{\leq {\rm th}}/n_{\rm fin} \rangle$; and (c) $\langle \tau_{\leq {\rm th}} \rangle$ and $\langle \tau_{\leq {\rm th}}/\tau_M^* \rangle$ are shown.